Experimental study of anomalous heating and trap instabilities in a microscopic ^{137}Ba ion trap

Ralph G. DeVoe and Christian Kurtsiefer
IBM Almaden Research Center, San Jose, California 95120
(Received 26 November 2001; published 13 June 2002)

A single $^{137}Ba^{+}$ ion has been laser cooled to the first few vibrational states of an 80-μm radius rf quadrupole trap. Initial measurements showed no anomalous heating of the vibrational phonon for observation times up to 1 ms, corresponding to a heating rate less than 3.3 phonons/ms at a 95% confidence level. Subsequently we observed the growth of large and unstable bias voltages that were correlated with exposure to the atomic beam. After loading over 250 ions over a period of 720 days the trap became unstable, with ion lifetimes <1 min. A possible connection between this trap instability and anomalous heating observed in quantum computation experiments is discussed. An isotopically selectively laser cooling method was used to refine ^{137}Ba ions out of a naturally abundant cloud.

DOI: 10.1103/PhysRevA.65.063407 PACS number(s): 32.80.Pj, 39.10.+j, 42.50.Vk

I. INTRODUCTION

Anomalous heating of the vibrational states of trapped ions has become one of the most important experimental obstacles to realizing of the Cirac-Zoller model [1] of quantum computation. In this model, ions are laser cooled to the quantum-mechanical ground vibrational state of an rf quadrupole trap. The center-of-mass phonon is used as a quantum communications channel to transmit information from one ion to another and to perform logical operations. The superposition of $n=0$ and $n=1$ states that is used to transmit quantum information is destroyed by any process that heats the ion, where n is the phonon quantum number. Since quantum gate operations take on the order of 10 μs, phonon lifetimes >1 ms are needed to make accurate tests of quantum logic, even for a few ions. Initial expectations based on experiments with millimeter scale traps were that phonon lifetimes of 1 s or more would be easily achieved. However, the first experimental test [2,3] of the Cirac-Zoller model showed a phonon lifetime of only 1 ms in a microtrap of radius 170 μm. Subsequent analysis [4,6,7] revealed that this anomalous decay could not be explained by Johnson noise, black body radiation, or any other fundamental mechanism. Experiments comparing the heating rates of symmetric and antisymmetric modes of a two ion crystal have shown [8] that the heating is due to a spatially uniform but temporally fluctuating electric field of about 1 mV/cm [5,9]. Further work comparing anomalous heating rates in six traps [9] with radii varying from 170 to 395 μm showed that the heating rate increased as d^{-4}. This dependence is consistent with a model in that the electric-field noise at the ion is due to fluctuating patch potentials on the electrodes, where the patch size is much smaller than the electrode dimension so that fluctuations in different parts of the electrodes are uncorrelated. Note that long phonon lifetimes of 200 ms have been observed in a larger trap of 700-μm radius, consistent with the d^{-4} relation observed above [10].

In this paper we study the trapping and heating of a single $^{137}Ba^{+}$ ion in a trap of 80-μm radius, which is 2–10 times smaller than other traps used in quantum computation. The original intention was that the small size of the trap would generate large phonon heating rates due to the d^{-4} law mentioned above, which allow experiments to reveal the physical mechanism. The results were unexpected in that the stability of the trapped ion deteriorated with time. Early in the experiment measurements of the height of the phonon sidebands for 1-ms delay showed no heating, which yielded a two standard deviation lower limit on the phonon lifetime of 300 μs. Given the scaling of the heating rate with d^{-4} and ion mass, this result is not in conflict with previous measurements on [9] Be or [10] Ca. In later work the trap became so unstable that phonon sidebands could not be measured, due to the short ion lifetime and fluctuating contact potentials. The trap stability continued to deteriorate until the ion lifetime was consistently less than 1 min. A factor of 2–4 increase in phonon heating rate over a 2-yr period has been observed previously [9] in Be, but not the loss of functionality reported here. We speculate in the conclusion, that both anomalous heating and the loss of trap stability are due to the accumulation of contaminants from the atomic beam on the trap electrodes and that this is the origin of the fluctating patch potentials inferred by Wineland *et al.* Since there is currently no accepted model for the physical mechanism underlying anomalous heating, establishing a hypothesis is necessary for determining a definitive experiment.

II. EXPERIMENT

This overall concept of the experiment is similar to that of Ref. [2] in that the qubit consists of two ground-state hyperfine levels that are driven by a pair of counterpropagating Raman beams. $^{137}Ba^{+}$ does not have a quasi-two-level system, useful for quantum state measurements, in the $S_{1/2}$ to $P_{1/2}$ system but does possess a metastable $D_{3/2}$ state with a long lifetime. A quasi-two-level system is available in the 455 nm $S_{1/2}$ to $P_{3/2}$ system, but this creates additional problems because of the $D_{3/2}$ and $D_{5/2}$ states at 585 and 614 nm, respectively, which at present can only be excited with dye lasers. Instead, we use the 493 nm $S_{1/2}$ to $P_{1/2}$ transition for cooling and optical pumping, and shelve the ion into the $D_{3/2}$ state at 650 nm for quantum state readout.

The hyperfine structure of the $^{137}Ba^{+}$ ion, which has nuclear spin $I=3/2$, is shown in Fig. 1. The $S_{1/2}$ and $P_{1/2}$ states have $F=1$ and $F=2$ sublevels, with spacings of

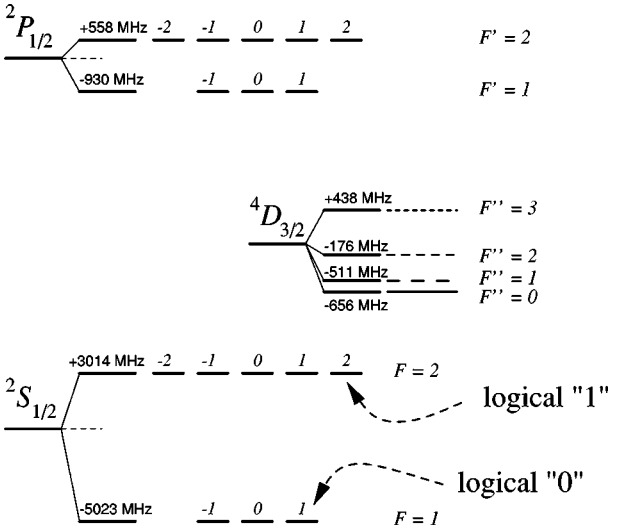

FIG. 1. The energy levels of the ^{137}Ba ion. The $S_{1/2}$, $P_{1/2}$, and $D_{3/2}$ states have different scales.

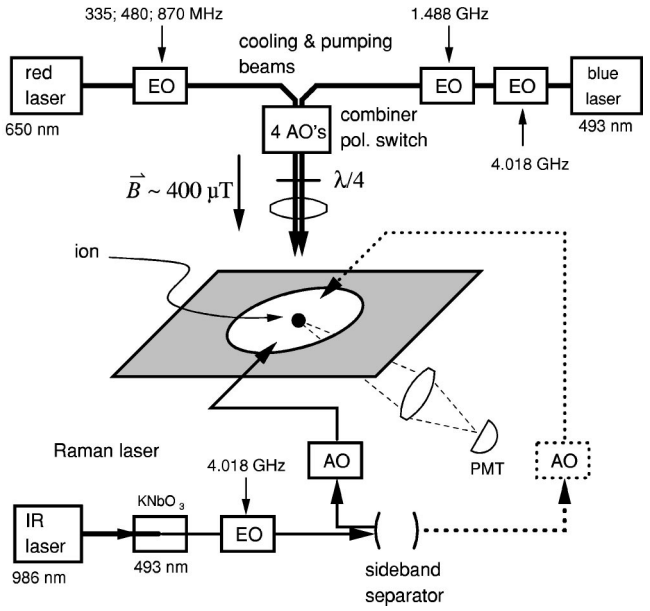

FIG. 2. The layout of the experiment. The circular aperture in the center is a schematic representation of the ion trap, with the vacuum tank not shown. Also not shown is a second ion trap of 5 mm diameter containing a single ^{137}Ba atom used as a frequency reference.

8037.742 MHz and 1488 MHz, respectively. The ground-state splitting has been measured with errors <1 ppm in a cloud of trapped ions [11] by microwave-optical double resonance, while the *P* and *D* state splittings have been measured in fast ion beams [12,13] with accuracies on the order of 1 MHz. The $D_{3/2}$ state has $F=0,1,2$, and 3 sublevels with hyperfine shifts of -655 MHz, -511 MHz, -176 MHz, and $+438$ MHz, corresponding to magnetic and electric quadrupole hyperfine interaction constants A_J and B_J equal to 189.73 MHz and 44.55 MHz, respectively. For convenience we designate the *S*, *P*, and *D* state total angular momentum as F,F', and F'', respectively.

A. Ion traps and laser cooling

The apparatus is shown in Fig. 2. The system comprises two ion traps, a large (5 mm) trap of conventional design that is used as resonance lamp for accurately tuning the laser frequencies, and a small planar trap [14,15] of 80-μm radius that provides high phonon frequencies useful for quantum logic. Doppler cooling is provided by a 493-nm beam together with a copropagating 650-nm beam that is used to prevent the accumulation of population in the $D_{3/2}$ state and also for shelving. The 493-nm light is generated by a home-built Coumarin 480 dye laser pumped by 408-nm Kr ion laser. The dye laser is servolocked to a temperature regulated vacuum interferometer using a 50-cm Zerodur cylinder as the primary length reference. The 650-nm light is generated by an external grating diode laser locked to a similar reference cavity. Long term stability is better than 1 MHz over a period of months as measured by the repeatability of the *S-P-D* two-photon resonance discussed below.

The 493-nm laser carrier is tuned to the midpoint of the $F=1$ and $F=2$ states and sidebands at ± 4018.370 MHz are generated by a microwave resonant-cavity electro-optic phase modulator driven by about 0.7 W of rf so that the carrier and first sidebands have approximately equal amplitudes. For Doppler cooling, the laser sidebands are resonated with the $F'=1$ level of the $P_{1/2}$ state. An additional microwave phase modulator driven at 1488 MHz is used when necessary to excite the $F'=2$ level, for example, for optical pumping or shelving to the $D_{3/2}$ state.

The primary Doppler cooling beam is inclined at an angle of 20° to the *Z* axis of the trap, parallel to an applied magnetic field of 4 G. The polarization of the blue and red beams can be switched in about 20 ns between σ^+ and σ^-. Polarization switching is accomplished by a system of acousto-optic modulators, quarter-wave plates, and beam combiners. The beam is focused to a 20-μm radius in the center of trap so that at resonance a few hundred nanowatts of blue light is sufficient to saturate the transition. For σ^+ polarization the 493-nm laser will optically pump the ion into a linear combination of the $|F,M_F\rangle=|1,1\rangle,|2,1\rangle$, and $|2,2\rangle$ states in a few *P* state lifetimes (7.92 ns). The laser cooling is sustained initially by switching back and forth between σ^+ and σ^- at every 100 ns. Faster switching speeds did not increase the flourescence rate or lead to colder ions. The primary Doppler beam does not provide optimum cooling for the *X* and *Y* axes because it is nearly perpendicular to them, since the cooling rate $\propto 1/\sin^2\theta$, where $\theta=20°$ [20,21]. Hence a secondary Doppler beam, inclined at 55° to the primary, is used to cool the *X* and *Y* axes to near the Doppler limit. The secondary beam is oblique to the axis of quantization, does not optically pump the ion, and provides steady-steady laser cooling without the need to switch polarizations.

We chose the $|F,M_F\rangle=|2,2\rangle$ and the $|F,M_F\rangle=|1,1\rangle$ states to define the qubit. The ion was prepared by optically pumping it into the former. This was achieved by setting the primary Doppler beam to σ^+, turning off the secondary beam, and turning on the 1488-MHz modulator, so that a sideband of the 493-nm light was resonant with the $S_{1/2}$ to

$P_{1/2}\,|F',M_F'\rangle=|2,2\rangle$ transitions. Since all transitions except those starting with the $|F,M_F\rangle=|2,2\rangle$ are excited, population is pumped into this state.

The $P_{1/2}$ state decays to the $D_{3/2}$ state with a branching ratio of 30%. *D-P* transitions must be continuously driven to avoid population accumulation due to the 47 s lifetime of this state. The $F'=1$ state will decay only to the $F''=0,1$, and 2 while the $F'=2$ state will decay to the $F''=1,2$, and 3, due to the $\Delta F=1$ rule. All four *D* sublevels must, therefore, be excited. A wideband traveling-wave electro-optic modulator was used to sequentially excite each state every 100 ns. For Doppler cooling the 650-nm laser carrier is resonated with the most heavily populated state, the $F''=2$ state and sidebands at 335 MHz and 480 MHz are used to empty the $F''=1$ and 0 states, respectively. For optical pumping, an additional rf pulse is applied at 870 MHz to empty the $F''=3$ level via the $F'=2$ level. These and other acousto-optic and electro-optic modulators are controlled by a 32 channel digital programmer.

B. Raman excitation and shelving by stimulated Raman adiabatic rapid passage

Raman transitions between the $|F,M_F\rangle=|2,2\rangle$ and the $|F,M_F\rangle=|1,1\rangle$ states are produced by two additional laser beams detuned by several GHz from the $P_{1/2}$ state and with a frequency difference equal to the 8037-MHz hyperfine spacing. The beams are generated by a third laser sysem based on a 1/2-w 986-nm source, consisting of a diode laser followed by a tapered amplifier. A 493-nm light is generated by a resonant-cavity doubler using $KNbO_3$ that produces 3 mW of second harmonic from 70 mW of fundamental. The two Raman frequencies are generated by a microwave phase modulator identical to the one used for Doppler cooling. Because of the short duty cycle of the Raman pulses, this modulator can be driven to null the carrier (modulation index $\beta=2.4$) using 7-W pulses of 4018-MHz rf. This reduces the chance of a spurious resonance of the carrier with the ion. The two sidebands enter a plane parallel optical cavity of 16-GHz free spectral range that reflects the lower sideband and transmits the upper. Less than 5% of the upper sideband remains in the reflected beam when resonant. The cavity is servocontrolled to the upper sideband by a lock-in detector. The reflected and transmitted beams are then switched by acousto-optic modulators and focused to a 20-μm beam waist radius in a counterpropagating geometry in the vacuum chamber.

The stimulated Raman adiabatic rapid passage method [16] has been used to coherently transfer amplitudes from one level to another in molecules and atoms. Here, it is used to ''shelve'' an amplitude to a metastable state as originally discussed by Dehmelt [17]. When the atom is shelved, all flourescence ceases, while in the unshelved case, the atom will continue to emit spontaneous photons for many lifetimes. This is necessary to make a quantum state projection measurement of a single atom, given the photon collection efficiency is less than 10^{-2}. We coherently transfer the amplitude of the $|F,M_F\rangle=|1,1\rangle$ level of the *S* state to the $|F'',m_{F''}\rangle=|3,3\rangle$ sublevel of the metastable *D* state, using the $|F',m_{F'}\rangle=|2,2\rangle$ level of the *P* state as the resonant ''dark'' state. The σ^+ and σ^- polarizations of the blue and red lasers are selected to excite this $\Delta F=2,\Delta M_F=2$ transition. (The red polarization is σ^-, since it stimulates the emission of a σ^- photon, increasing the angular momentum of the atom). Since the Doppler cooling beams are normally tuned about 20 MHz below resonance to the $F'=1$ hyperfine level of the *P* state, the 1488 MHz modulator is turned on so that the upper sideband resonates with the $F'=2$ level. The acousto-optic modulators are driven to produce complementary linear ramps by driving rf modulator diodes with properly shaped pulses. Overall transfer efficiency is over 50%.

C. Isotopic purification and the ^{137}Ba atomic beam

Barium has seven stable isotopes, with masses of 130, 132, 134, 135, 136, 137, and 138 amu and abundances of 0.1%, 0.1%, 2.5%, 6.6%, 7.8%, 11.3%, and 71.7%, respectively. The even isotopes have spin zero and ^{135}Ba and ^{137}Ba both have spin 3/2. ^{137}Ba was chosen because of its abundance and because its isotope shift facilitates isotopic purification by selective laser cooling. Even if an enriched oven is used to load the ion trap and even if the number of trapped ions is small, it is nevertheless likely that occasionally one of the more abundant $I=0$ isotopes will be loaded. This method permits such ions to be ejected from the trap.

The large (5 mm diameter) ion trap was operated with an unenriched barium atomic beam and is used as a single-ion frequency standard for setting the 493- and 650-nm lasers to the optimum ion loading frequencies. We distill a single $^{137}Ba^+$ from a cloud of naturally abundant isotopes by using the 493-nm laser carrier, which is nonresonant with any $^{137}Ba^+$ transition, to heat the $I=0$ isotopes. When the ± 4-GHz sidebands are in resonance with the $^{137}Ba^+$ hyperfine levels, the carrier lies from 350 MHz to 225 MHz above the transitions of the five $I=0$ isotopes, heating them into large orbits. These ions can then be ejected from the trap by reducing the trap depth with a dc potential (''a'' term in the Mathieu equations). In this way a single $^{137}Ba^+$ ion may be distilled from dozens of ions in a few minutes. Once loaded this trap holds ions for several months without laser cooling. This is consistent with the excellent vacuum resulting from more than ten years of continuous operation at pressures below 5×10^{-10} Torr. During the first few years the ion lifetime was less than 24 h, presumably due to a small partial pressure of CO_2 and other gases that can form covalent bonds during collisions.

The 80-μm trap was loaded by an enriched atomic beam containing 85% ^{137}Ba . The beam was generated by a double oven that provides fewer contaminants and better control of atomic flux than a conventional device. The first part of the oven generates free ^{137}Ba by a chemical reaction of $^{137}BaCO_3$ with tantalum powder at 1200 °C. The barium is sprayed onto the second part, called the hot plate, whose temperature is regulated to a few degrees celcius by a thermocouple. The trap is loaded by operating the hot plate at 370–380 ° C, which permits precise regulation of the vapor pressure. Contaminants in the atomic beam are reduced by two mechanisms. First, there is no line-of-sight path between

the first oven and the trap so that high-temperature byproducts of the reaction do not reach the trap directly. Second, any contaminants that reach the hot plate will tend not to reach the trap because those whose vapor pressure is higher than 380 °C will never leave the hot plate, while those whose vapor pressure is lower will all be removed the first time it is operated. It acts as a vapor pressure filter.

It is necessary to generate ^{137}Ba by a chemical reaction in high vacuum because free Ba reacts quickly with the atmosphere to produce BaO and other compounds that are not readily dissociated. The first oven is initially heated to 1100 °C while connected to a turbo pump at 10^{-4} Torr before bake out. The$^{137}BaCO_3$ evolves CO_2 gas so that only^{137}BaO remains. The chamber is then baked at 250 °C for 24 h. When the trap is ready to use, the mixture of BaO and Ta powder is heated to 1200 °C to form free ^{137}Ba which coats the hot plate. Once the hot plate is charged it can be used over a period of several months to load from 10–30 ions. The hot plate may be recharged an indefinite number of times by reheating the first oven. In practice over 300 ions were loaded over a period of two years without breaking vacuum.

This is in contrast to another widely used method of generating free Ba from an exothermic reaction of $BaAl_4$ with Ni at 800 °C. At this temperature Al has a high vapor pressure and it is likely that the atomic beam contains Al and other impurities as well as Ba. The stability of ions loaded from such an oven was grossly different from that of the refined oven, as discussed below.

III. CONTACT POTENTIALS AND TRAP INSTABILITY

It is well-known ion traps have stray electric fields in their interior that can bias an ion off the center of the trap. Most ion traps have ''compensation electrodes'' that are used to cancel these fields and return the ion to the center of the trap. Laser cooling to the ground state usually requires this. The problem has been so significant that Dehmelt has constructed a microscopic Paul-Straubel trap [19] that could be heated to up to 1000 °C to evaporate the Ba deposited by the atomic beam, which reduced the compensation voltage significantly. In the present experiment the compensation voltage C_v was measured over two and half years and correlated with the onset of trap instabilities.

The above system was used to load ≈ 311 ions over a period of 798 days. During the first 690 days and 240 ions the trap behaved in a stable and repeatable manner. Specifically, the bias or compensation voltage remained stable to about ± 10 V for the duration of datataking, typically 6–10 h. Furthermore, ions once loaded remained in the trap for as long as desired. Unexplained ion loss occurred less than three times during this entire period, comprising several thousand hours of datataking, indicating a mean ion life greater than 500 h. The compensation voltage increased over a period of months as it was exposed to the atomic beam and dropped during periods of inactivity, as shown in Fig. 3.

This behavior changed gradually starting about day 690 (where day 1 was April 5, 1999). Over the course of the next 90 days, the mean ion lifetime dropped to several hours and

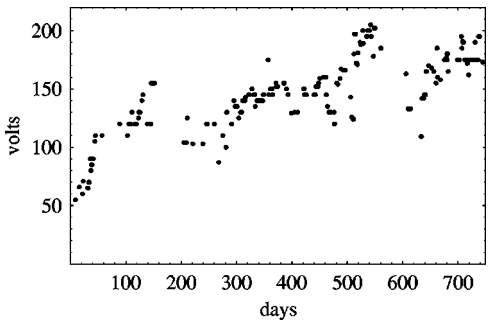

FIG. 3. A plot of the compensation voltage C_V over a period of 700 days. Note the rapid increase during periods of heavy exposure to the atomic beam and the drop during periods of inactivity. During the last few months C_V varied unpredictably during the course of each experiment and finally made it impossible to trap the ion more than a few minutes.

the compensation voltage began to drift during the experiment. During the last 20 days of the experiment the ion lifetime dropped to about 1/2 h and the compensation voltage became so unstable that the ion flourescence as viewed on an imaging photomultiplier showed visible fluctuations in intensity over a period of several minutes. At the end of this period the compensation voltage changed so rapidly and with such large values that it could not be set properly and ion loss followed. Because of the gradual onset of this behavior there was sufficient time to test the hardware to eliminate a trivial origin. Furthermore, when the vacuum chamber was opened and the barium oven replaced without touching the trap long ion lifetimes and small, stable compensation voltages returned. It appears that exposure to air and the subsequent bake out ''cleans'' the trap of whatever causes the stray fields. Replacment of the double oven by a similar device that had been more carefully cleaned showed about half the rate of rise of C_v.

Previous work with the same trap but an unrefined Ni $BaAl_4$ source showed completely different behavior. C_V took both positive and negative values and subsequent loads differed by ± 100 V or more. While there was a general increase in $|C_V|$ with time the regular behavior of Fig. 3 was not apparent. After 20–30 ions the trap abruptly stopped loading at a large positive or negative value of C_V. This behavior was also reset after exposure to air.

Experiments have shown that the trap instability is not due to charging of the trap insulators by the electron beam. First, the electron beam was turned on at about 20% of the loading value while an ion was being observed in the trap, without changing the compensation voltage. Second, an electron current about ten times the loading value was left on the trap for about ten times the usual length of a load, which also had little effect.

IV. SEARCH FOR HEATING OF VIBRATIONAL PHONONS

It is customary to consider two ground state-levels of a trapped ion driven by Raman beams of Rabi frequencies Ω_1 and Ω_2 as forming an effective two level system with a Rabi

frequency equal to $\Omega_1\Omega_2/\Delta$, where Δ is the detuning from resonance. For a $\Delta n=-1$ transition [4,22,23] the effective Rabi frequency becomes

$$\eta_i\sqrt{n}\,\frac{\Omega_1\Omega_2}{\Delta} \tag{1}$$

with Lamb-Dicke factor

$$\eta_i=(\mathbf{k_1}-\mathbf{k_2})\cdot\hat{n}_\mathbf{i}\sqrt{\frac{\hbar}{2\,\mathrm{m}\omega_i}}, \tag{2}$$

where $\mathbf{k}_{1,2}$ are the wave vectors of beams 1 and 2, $\hat{\mathbf{n}}_\mathbf{i}$ is a unit vector pointing in the direction of the ith vibrational mode ω_i, and m is the mass of the ion. For $\Delta n=+1$ transitions, the factor $\sqrt{n}$ is replaced by $\sqrt{n+1}$. The effective two-level system is also known [4,22,23] to have a light shift term

$$\frac{\Omega_1^2-\Omega_2^2}{\Delta}. \tag{3}$$

Note that for the $\Delta n=0$ transition the light shifts are always smaller than the linewidth provided that $\Omega_1\approx\Omega_2$. This follows from comparing Eq. (3) to the effective Rabi frequency $\Omega_1\Omega_2/\Delta$. This is not true for the $\Delta n\pm1$ transitions since here the effective Rabi frequency is reduced by the factor $\eta_i\sqrt{n}$ but the light shifts are not. This is important for heavy ions, where $\eta_i\leqslant0.1$. In this experiment it was necessary to empirically adjust the light shifts to obtain Fourier-limited phonon signals. This was done by observing the $\Delta n=0$ transition for Raman pulse widths varying from 600 ns to 40 μs. The effective Rabi frequency $\Omega_1\Omega_2/\Delta$ was adjusted for a π pulse in each case, while holding the ratio of the powers in beams 1 and 2 constant. If Ω_1 and Ω_2 are unequal, the center of the resonance will shift as the pulse width is varied. The relative strengths of the two beams can then be adjusted until all pulse widths have the same center frequency.

The Raman signals were observed by a pulse sequence containing 4 steps. Step 1 comprised Doppler cooling resonant with the $P_{1/2}$ $F'=1$ state and lasted for 50 μs. The primary and auxiliary blue beams were turned on while the red beam was resonated with the $D_{3/2}$ $F''=2$ level. A rf sidebands at 335 MHz and 480 MHz depopulated the $F''=0$ and 2 states as described above. Step 2 lasted 5 μs and optically pumped the ion into the $|F,M_F\rangle=|2,2\rangle$ state. Here the 1488-MHz modulator was turned on to resonate with the $F'=2$ level while the auxiliary blue beam was turned off and the red laser remained on. Step 3 drove the Raman transitions from the $|F,M_F\rangle=|2,2\rangle$ state to the $|1,1\rangle$ state and lasted from 600 ns to 40 μs. Here all beams were turned off except the two Raman beams. Step 4 read out the population of the $|F,M_F\rangle=|1,1\rangle$ state by turning on the primary blue beam and the 1488-MHz modulator so that the strong transition $|F,M_F\rangle=|1,1\rangle$ to $|F',M_{F'}\rangle=|2,2\rangle$ was driven. Shelving was not used for these tests and Step 4 lasted only 500 ns, which generated a Raman signal of 20–30 counts/s, sufficient to determine the center frequency in a few minutes. Figure 4a–4(c) show the Raman signal for pulse widths of 600 ns, 5 μs, and 40 μs, which are fit to the effective two-level theory [4,22,23]. Note the quality of this fit over the 66 is to 1 ratio and that no light shifts are apparent.

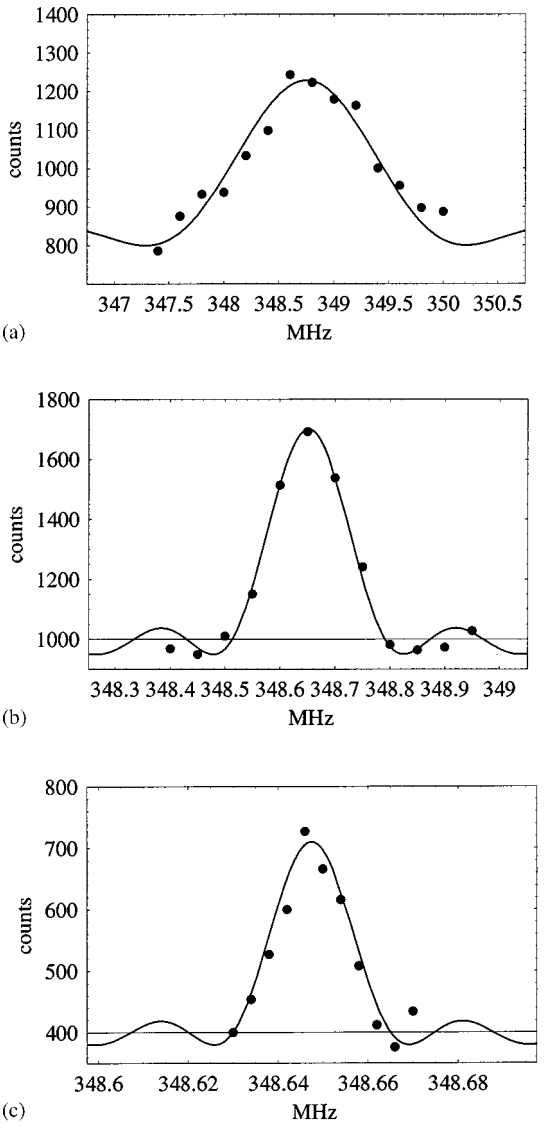

FIG. 4. Showing the agreement of the Raman carrier signal with the Fourier-limited theory for pulse widths of (a) 600 nS, (b) 5 μs, and (c) 40 μs. The fact that all the resonance curves have the same center frequency shows that the light shifts are equal, as discussed in the text.

The ion trap [14,15] has near-circular symmetry with $\omega_x\approx\omega_y\approx4$ MHz and $\omega_z=8$ MHz at the operating voltage of 600-V peak. The Lamb-Dicke factors $(\eta_x,\eta_y,\eta_z)=(0.032,0.032,0.045)$ indicate that the $\Delta n=\pm1$ phonon sidebands will be significantly weaker than the $\Delta n=0$ carrier. To compensate for this, two sets of data were taken simultaneously, one with a Raman pulse of 1 μs and another with 5 μs. The Raman intensity was set to give a π pulse for the $\Delta n=0$ transition at 1-μs pulse width. The 5-μs data then gave a $5\sqrt{n_i}\eta_i$ π pulse for the phonons, which are shown in Fig. 5.

Shelving was necessary for the heating measurement since the heating times of upto 1 ms reduced the data rate by a factor of 20. Shelving added steps 5 and 6 to the pulse

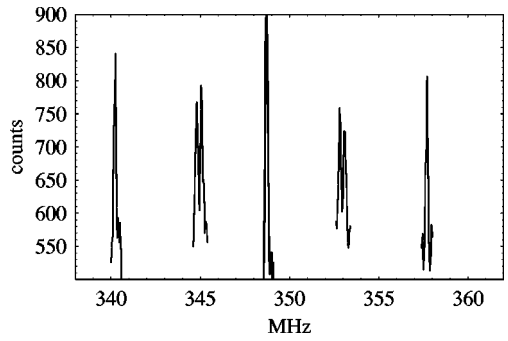

FIG. 5. The phonon spectrum of the trap. Note that the degeneracy of the x and y phonons is lifted by a slight ellipticity of the near-circular trap apertures. The frequency difference of the two Raman beams is 7680 MHz plus the tuning frequency given on the x axis.

sequence, where step 5 transferred the population of the $|F,M_F\rangle=|1,1\rangle$ state to the $D_{3/2}\,|3,3\rangle$ state via the $P_{1/2}\,|2,2\rangle$ state as described above. Step 6 then read out this state for a period of 15 μs by turning on the σ^+ blue beam, turning off the 1488-MHz modulator, and turning on the red laser and the 335- and 480-MHz sidebands to depopulate all the metastable levels except the $|3,3\rangle$ shelving state. The limiting factor in this was off-resonant excitation of the shelving state by the red light used to depopulate the $F''=0,1$, and 2 levels. In early experiments shelving lifetimes of over 200 μs were common, but the data here used higher red powers that limited the shelving lifetime to about 30 μs. The shelved data rate was 200–400 counts/s at the fastest decoherence times, dropping to 10 counts/s for 1 ms delays.

Heating data were taken by inserting a dead time ranging from 50 μs to 1 ms after the optical pumping in step 2. The dead time consisted of turning off all acousto-optic and electro-optic modulators. The phonon sidebands were measured before and after the dead time. The signature of heating is that the delayed sideband would be larger than the prompt sideband. The data of Fig. 6 show no sign of heating any delay time. These data were fit to the theoretical signal (Refs. [4,22,23]) using a nonlinear regression routine. The background counts and the depth of the resonance were treated as free parameters while the width and center frequency were constrained. The χ^2 per degree of freedom for the prompt and delayed phonons of Figs. 6(b), 6(c), and 6(d) were 1.7, 0.5, 1.0, 1.0, 1.3, and 1.3 indicative of an excellent fit. By increasing the height of the theoretical signal for the delayed data until the χ^2 increased by the requisite amount, we derive that heating rates >3.3 phonons/ms, or a phonon lifetime <300 μs, can be excluded with 95% confidence (two standard deviations). Both Figs. 6(c) and 6(d) have the same statistical power. This result is not in conflict with earlier measurements of phonon lifetime in Be and Ca, which scale approximately [5,9] as m/d^4. For example, the 1-ms lifetime in a 170 μm trap using ^{9}Be scales to 310 μs for ^{137}Ba and $d=80$ μm.

V. CONCLUSION

It is important to place these results in the context of previous work on anomalous heating. The NIST study included the construction of six different traps over a period of five years and concluded [9] ''Since we have not identified

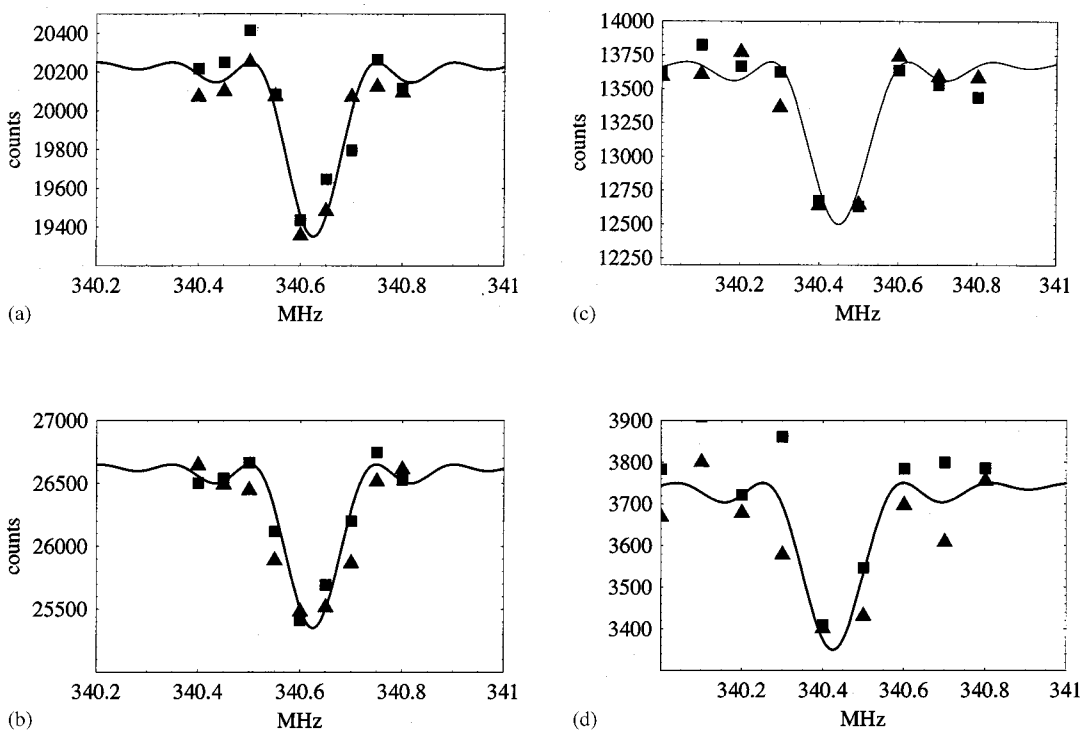

FIG. 6. The shelved axial lower phonon sideband (z axis) shown before a decoherence interval (boxes) and after (triangles) for dead times of (a) 100 μs, (b) 200 μs, (c) 400 μs, and (d) 1000 μs. No sign of anomalous decoherence is apparent at any delay time.

the mechanism for the observed heating, it is difficult to say what path should be taken to correct it.'' And '' . . . systematic studies of the dependence of heating rate on various trap properties are difficult, since this often requires the construction of an entirely new trap apparatus, which may have different values of properties not under study.'' An evaluation of our experimental results suggests a hypothesis that can be tested in subsequent work.

The most surprising result of our experiment is that the stability of the trap degrades over time. Ion lifetime in the trap was initially >500 h but dropped to less than 1 min after two years of operation comprising over 300 single-ion experiments. We speculate that this is due to contamination of the trap surfaces by the atomic beam. The hypothetical physical mechanism is that the atomic beam deposits either ^{137}Ba or other impurities on the trap electrodes creating contact potentials, which fluctuate either due to movement of the adsorbates across the surface or, on a slower time scale, due to chemical reactions with the background gas (see also Ref. [18].) In such a model fluctuations in different parts of the trap are uncorrelated, consistent with the d^{-4} patch potential model of Ref. [9]. The significance of the >300 μs phonon lifetime measured above is that there was relatively little heating when the trap was clean early in the experiment. The later observations of ion loss are then manifestations of an extremely large and irregular heating rate. Note that this ion trap has a depth of $\approx 10^7$ vibrational levels so that if the instability is driven by electric-field fluctuations as hypothesized above, large phonon heating rates must accompany the instability.

The primary evidence for this model comes from the correlation between the stability of the compensation voltage C_V and the ion lifetime. Early in the experiment, when the relatively long phonon lifetimes of Fig. 6 were recorded, the flourescence rate at resonance (≈ 11 KHz) could be maintained with a constant value of C_V for an entire run of 6–10 h. As the experiment progressed C_V needed to be adjusted at progressively more frequent intervals. At the end, the value of C_V could not be adjusted fast enough (every few seconds) to maintain a constant count rate and ion loss followed quickly. While it is possible that the fluctuating value of C_V could be unrelated to the ion loss (which might be due, for example, to momentary loss of rf drive), several months were spent in excluding hardware artifacts as a cause. No changes in the basic operating parameters of the trap were observed during the experiment other than C_V.

The idea that exposure to the atomic beam creates increasing bias fields in the trap is also supported by C_V history of Fig. 3. During periods of intense use, C_V increases rapidly. During periods of inactivity, C_V declines with an approximate half-life of three to six months, perhaps due to chemical reactions with the background gas. Again, it is possible that the behavior of C_V is unrelated to total atomic beam dose, and, for example, is due to electron-beam charging of insulators, but no effect of the electron beam on C_V has been found in the experiments noted above. Additional evidence relating C_V to the atomic beam is provided by earlier experiments with a relatively dirty Ba beam resulting from exothermic reactions in $BaNiAl_4$. As noted above, this source produced a larger and more erratic C_V record than that of refined source, with the rest of the apparatus identical.

Several definitive but difficult experiments are possible. Shielding the trap from the atomic beam would require a highly collimated atomic beam and a small aperture, due to the 80-μm radius of the trap. Alternatively, the trap could be heated [19] to 400 °C, where surface Ba evaporates in a few seconds. Another approach [24], originally intended to protect mirror surfaces, is to use a small linear trap in that the ions are loaded in a separate part of the trap and moved into an operating region not accessible to the beam. If our hypothesis is correct, both anomalous heating and time-dependent trap instabilities would be absent from such systems.

[1] J.I. Cirac and P. Zoller, Phys. Rev. Lett. **74**, 4091 (1995).
[2] C. Monroe, D.M. Meekhof, B.E. King, S.R. Jefferts, W.M. Itano, D.J. Wineland, and P. Gould, Phys. Rev. Lett. **75**, 4011 (1995).
[3] C. Monroe, D.M. Meekhof, B.E. King, W.M. Itano, and D.J. Wineland, Phys. Rev. Lett. **75**, 4714 (1995).
[4] D.J. Wineland, C. Monroe, W.M. Itano, D. Leibfried, B.E. King, and D.M. Meekhof, J. Res. Natl. Inst. Stand. Technol. **103**, 259 (1998).
[5] D.F.V. James, Phys. Rev. A **81**, 317 (1998).
[6] S.K. Lamoreaux, Phys. Rev. Lett. **56**, 4970 (1997).
[7] C. Henkel and M. Wilkens, Europhys. Lett. **47**, 414 (1999).
[8] B.E. King, C.S. Wood, C.J. Myatt, Q.A. Turchette, D. Leibfried, W.M. Itano, C. Monroe, and D.J. Wineland, Phys. Rev. Lett. **81**, 1525 (1998).
[9] Q.A. Turchette, D. Kielpinski, B.E. King, D. Leibfried, D.M. Meekhof, C.J. Myatt, M.A. Rowe, C.A. Sackett, C.S. Wood, W.M. Itano, C. Monroe, and D.J. Wineland, Phys. Rev. A **61**, 063418 (2000).
[10] Ch. Roos, Th. Zeiger, H. Rhode, H.C. Nagerl, J. Eschner, D. Leibfried, F. Schmidt-Kaler, and R. Blatt, Phys. Rev. Lett. **83**, 4713 (1999).
[11] R. Blatt and G. Werth, Phys. Rev. A **25**, 1476 (1982).
[12] R.E. Silverans, G. Borghs, P. DeBisschop, and M. Van Hove, Phys. Rev. A **33**, 2117 (1986).
[13] P. Villemoes, A. Arnesen, F. Heijkenskjold, and A. Wannstrom, J. Phys. B **26**, 4289 (1993).
[14] R.G. Brewer, R.G. DeVoe, and R. Kallenbach, Phys. Rev. A **46**, R6781 (1992).
[15] R.G. DeVoe and R.G. Brewer, Phys. Rev. Lett. **76**, 2049 (1996).
[16] J.W. Martin, B.W. Shore, and K. Bergmann, Phys. Rev. A **54**, 1556 (1996).
[17] H. Dehmelt, Rev. Mod. Phys. **62**, 525 (1990).
[18] R.G. DeVoe, Phys. Rev. Lett. (to be published).
[19] N. Yu, W. Nagourney, and H. Dehmelt, J. Appl. Phys. **69**, 3779 (1991).

[20] D.J. Wineland and W.M. Itano, Phys. Rev. A **20**, 1521 (1979); **25**, 35 (1982).
[21] S. Stenholm, Rev. Mod. Phys. **58**, 699 (1986).
[22] J. Steinbach, J. Twamley, and P.L. Knight, Phys. Rev. A **56**, 4815 (1997).
[23] L. Davidovich, M. Orszag, and N. Zagury, Phys. Rev. A **54**, 5118 (1996).
[24] G.R. Guthoerlein, M. Keller, K. Hayasaka, W. Lange, and H. Walther, Nature (London) **414**, 49 (2001).